2014 5th IEEE RAS & EMBS International Conference on
Biomedical Robotics and Biomechatronics (BioRob)
August 12-15, 2014. São Paulo, Brazil

# Driving Force Assistance Control for Wheelchair Operation Using an Exoskeletal Robot

Naoto Mizutani[1], Hirokazu Matsui[1], Ken'ichi Yano[1], Yasuyuki Kobayashi[2]

*Abstract*— **Cervical Cord Injury(CCI) causes a form of upper limb dysfunction. In an individual with C5-level CCI, which is the most frequent of all eight types of CCI, force can be applied in the direction of flexion by the biceps brachii, while extension force cannot be applied by the triceps brachii. Without the ability of the triceps brachii to exert this force, individuals with a C5-level CCI cannot propel a wheelchair along a carpet or sloping road. In this study, we developed a driving force assistance control system for wheelchair operation using an exoskeletal robot. We first analyzed the difference between the wheelchair operations of a healthy person and a C5-level CCI. We then designed a control model that included a user and a wheelchair. The wearer's arm was modeled as a two-link manipulator, and the extension force and hand position were estimated using the equation of motion. The estimated extension force was compared with the driving force required to operate a wheelchair with the target velocity defined at the time of flexion of an arm. We then applied the proposed method via an exoskeletal robot. The effectiveness of the proposed method is demonstrated by experimental of wheelchair operation with C5-level CCI.**

## I. INTRODUCTION

The number of disabled persons has been increasing every year. The disabilities include various kinds of dysfunctions of the upper extremities. Two-thirds of spinal cord injuries are caused by traffic accidents or by a fall from a high altitude. An individual with a cervical cord injury are forced to use a wheelchair due to an impairment of the inferior limbs. In addition, their trunks and upper limbs, including their fingers, can become paralyzed as their condition worsens. In recent years, it has been estimated in the U.S. that there are approximately 12,000 incidence of spinal cord injury every year. In an individual with a C5-level cervical cord injury (CCI), force can be applied in the direction of flexion by the biceps brachii muscle, but extension force cannot be applied due to paralysis of the triceps brachii muscle. And because these individual cannot hold the wheel rims of the wheelchair due to paralysis of the hand, they cannot operate the wheelchair like persons with healthy upper limbs. It is therefore difficult to propel a wheelchair across a carpet or up a slope, and the wheelchair velocity is very slow because the coasting span is quite short.

Electric and power-assisted wheelchairs can be used to expand the field of activities for individuals with a C5-leve CC. These wheelchairs can move without a user's driving force. With these wheelchairs, the user's field of activities increases. However, the activities of daily living that become difficult due to a poor extension force are not limited to wheelchair operation. For example, there are push movements such as pushing a door open and pushup operations to prevent bedsores. Therefore, even if these wheelchairs can expand the user's field of activities, if the operations that can be performed by users self are restricted, it is difficult to say that a user's sphere of activities spreads. If functions such as those of the triceps brachii muscle can be assisted and extension force can be applied, wheelchair operation and other activities of daily living can be performed by individuals and will lead to an expansion of the sphere of activities.

It would be desirable if a wearable support robot could be used to substitute for the muscular power lost as a result of a CCI. Research to estimate the user's motion using a pressure sensor or EMG sensor, and to assist motion by amplifying and assisting power has previously been carried out[1]-[9]. Morbi et al.[10] have amplified the value of a pressure sensor when a wearing person moves, applying a gain. In addition, Weiguang et al.[11] have selected the operation of four patterns beforehand, and have changed the motion of the device based on the value of the pressure sensor. In these previous studies, the assistive force and assist timing have been determined based on the value of a pressure sensor or EMG sensor, which is attached to a device. However, a patient who has muscle paralysis, like an individual with C5-level CCI, cannot apply force correctly in the direction which needs assistance. In addition, using only these sensors, it is difficult to judge whether the sensor's value was detected due to the motion of the user or to the influence of disturbance. Therefore, an assist system that can assist according to the user's motion by estimating the motion of an actual user's arm is needed. Furthermore, in previous studies, the motion fixed in advance has been performed by feed forward control. Therefore, the user cannot move freely while the device is moving. The device must successfully interpret the motion of the user's arm and be controlled by feedback. Because it is necessary to correctly interpret the motion of the user's arm, this motion is modeled, including a control system, and the support required to achieve suitable timing is offered by feedback not only a sensor value but the motion of the arm.

In the present study, we developed a driving force assistance system for wheelchair operation based on an upper limb model. First, motion of the arm at the time of wheelchair operation was modeled as a two-link manipulator, and the user's hand position and extension force were estimated using an equation of motion. The estimated extension

[1]N. Mizutani, H. Matsui and K. Yano are with the Department of Mechanical Engineering, Mie University, 1577 Kurimamachiyacho, Tsu, 514-8507, Japan yanolab@robot.mach.mie-u.ac.jp

[2]Y. Kobayashi is with LUMINOUS JAPAN CO.,LTD., 68 Hagae, Murakami, 959-3134, Japan

978-1-4799-3127-9/6/14/$31.00 ©2014 IEEE

force was then compared with the driving force required to operate a wheelchair with the target velocity defined at the time of flexion of an arm. We developed a system that can assist with problems of an insufficient driving force. The effectiveness of the proposed method for wheelchair operation with C5-level CCI was investigated.

## II. EXOSKELETAL ROBOT

### A. The Robot's Structure

A exoskeletal robot was developed to support individual with upper limb dysfunction. This robot is shown in Fig. 1. This robot was designed for prolonged use and operability. The input in the control is a pressure sensor installed in the forearms. This robot's schematic diagram is shown in Fig. 2. The forearm is a double structure composed of an inner part and an outer part. The inner part can move freely. Because the pressure sensor is sandwiched between the inner part and the outer part through the flat spring, the sensor is able to detect the wearer's motion for flexion and extension. A brushless DC 100W motor was used as an actuator. To relieve heat generated in this motor, this robot's frame is made by aluminum alloy. The specifications of this robot are shown in Table I. An allowance of about 8.0 [deg] was designed in the direction of adduction and abduction of the front arm in order not to encumber the motion of the frame of the front arm in the joint axis. We developed a special orthosis which is a part of the frame that adheres to the human body. The orthosis has a dual structure of both soft and hard material. The soft material is for fitting, and the hard material for power transmission. About a wearing part, the device is fixed by belts and this orthosis. The robot is designed in accordance with the wearer's physique to enhance the operability.

Fig. 1. Exoskeletal robot for the upper limb

TABLE I

SPECIFICATIONS OF THE DEVICE

| | |
|---|---|
| Weight | 855 [g] |
| Actuator's rated output | 100 [W] |
| Nominal torque | 5.26 [Nm] |
| Nominal speed | 475 [deg/s] |
| Range of movement | 135 [deg] |

### B. The Robot's Control System

The robot must not obstruct the wearer's motion in the range of motion which wearer can move freely. Therefore,

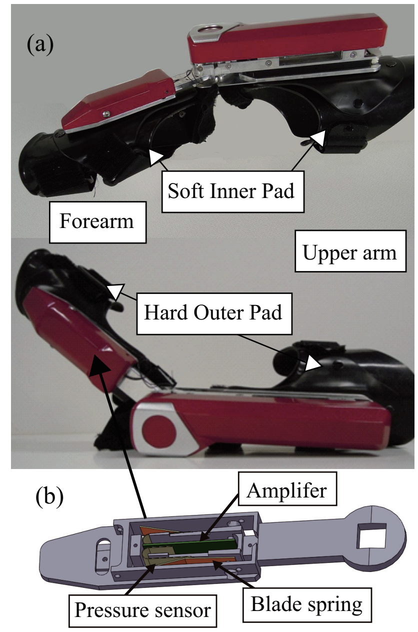


Fig. 2. (a) Whole device's structure, (b) Structure of sensor part

in order to follow the wearer's motion when the robot doesn't support, the robot is controlled by an admittance controller based on the information from the pressure sensor attached the forearm. The transfer function $G_A(s)$ is the admittance controller of the spring mass damper system as (1).

$$G_A(s) = \frac{1}{Ms^2 + Ds + K} \tag{1}$$

where $M$ is the inertia coefficient[$\mathrm{kgm^2}$], $D$ is the viscosity coefficient[$\mathrm{Nms/deg}$], and $K$ is the stiffness coefficient[$\mathrm{Nms/deg}$]. In addition, $D$ and $K$ are variable. $D$ is represented by (2).

$$D = \frac{D_{\mathrm{I}}}{\frac{|\dot{\theta}_h|}{A_{\mathrm{D}}} + 1} \tag{2}$$

where $D_{\mathrm{I}}$ is the initial viscosity coefficient[$\mathrm{Nms/deg}$], $A_{\mathrm{D}}$ is the viscosity decrease ration[-], and $|\dot{\theta}_h|$ is the angular velocity of the wearer's arm[$\mathrm{deg/s}$]. $|\dot{\theta}_h|$ is represented by (3). $f_{in}$ is the input from the pressure sensor after passing the filter[V] and is obtained for the joint angle of the free motion of the inner part to an outer part in the front arm dual structure of the wearable robot using the constant $A_{\mathrm{h}}$. Although the input of the pressure sensor is nonlinear, note that it is treated linearly in this research.

$$\dot{\theta}_{\mathrm{h}} = \frac{(f_{in}A_{\mathrm{h}} + \theta_m)s}{T_{\mathrm{h}}s + 1} \tag{3}$$

The wearer's elbow joint angle is the sum of the angle of the inner part and the joint angle of the outer part $\theta_m$. The joint angular velocity is obtained by derivation of the wearer's elbow joint angle. However, because signal noise becomes large, it passes the low pass filter of the first order leg of the time constant $1/T_{\mathrm{h}}$. $D$ is changed depending on the angular velocity of a wearer's arm $|\dot{\theta}_h|$[deg/s].

Therefore, operability is improved by increasing viscosity when the arm stops moving and decreasing it when the arm begins to move. In this research, $A_\mathrm{h}$=0.75, $T_\mathrm{h}$=0.01, $D_\mathrm{I}$=0.6, $A_\mathrm{D}$=50, $M$=1/25000. The angular limitation is set from the software and hardware for safety. The robot can only perform extension and flexion at a fixed angle. When the arm reaches the angle limit whether in flexion or extension, the motor is rapidly suspended, and the output and load becomes momentarily large. The virtual spring is set at each termination point in order to reduce the load of the motor. It is represented by (4) and (5).

$$K(\theta) = K_{\max}\frac{A_{sp}(\theta)}{A_{\mathrm{lg}}} \tag{4}$$

$$A_{sp} = \begin{cases} \theta_m + A_{\mathrm{lg}} & (\theta \geq -5) \\ 0 & (-5 > \theta > -115) \\ \theta_m + (120 - A_{\mathrm{lg}}) & (-115 \geq \theta) \end{cases} \tag{5}$$

The motion angle of the robot is taken as a positive value in the expansion direction and set from -120[deg] to 0.0[deg], which is the maximum expansion. In this research, $K_{\max} = 4.0$, $A_{\mathrm{lg}} = 5.0$ where $K_{\max}$ is the maximum value of input from the pressure sensor.

## III. ANALYSIS OF WHEELCHAIR OPERATION

Before designing a driving force assistance system, in order to check the driving force which an actual individual with C5-level CCI can apply, the wheelchair operation was analyzed. In doing so, we focused on the manipulating force ellipsoid (MFE) in order to quantitatively analyze the operator's force.

### A. The Manipulating Force Ellipsoid (MFE)

The relation between joint torque and hand force was analyzed using the concept of the MFE used by robotics. This approach involves evaluating a hand's manipulating force quantitatively from a kinematic perspective[12].

An arm with $n$ degrees of freedom is considered, with $\boldsymbol{f}$ being the force that a hand gives to an object, $\boldsymbol{\tau}$ being a $n$ dimension vector, the set of all the joint torques and $\boldsymbol{J}(\theta)$ being the Jacobi matrix. When an arm is not in a singular state, the relation between hand force and joint torque is as follows.

$$\boldsymbol{\tau} = \boldsymbol{J}^T(\boldsymbol{\theta})\boldsymbol{f} \tag{6}$$

All the sets of $\boldsymbol{f}$ that can be realized by using $\boldsymbol{\tau}$, which satisfies the Euclid norm $||\boldsymbol{\tau}|| = (\tau_1^2 + \tau_2^2 + \cdots + \tau_n^2)^{1/2} \leq 1$, becomes the following $m$ dimension ellipsoid.

$$\begin{aligned} ||\boldsymbol{\tau}|| &= \boldsymbol{\tau}^T\boldsymbol{\tau} \\ &= \boldsymbol{f}^T\boldsymbol{J}\boldsymbol{J}^T\boldsymbol{f} \leq 1 \end{aligned} \tag{7}$$

If the main radius of this ellipsoid is long, then a large hand force is exerted in the radial direction.

The principal axis of this ellipse is calculated as follows. The singular value analysis of $\boldsymbol{J}$ is as follows.

$$\boldsymbol{J} = \boldsymbol{U}\boldsymbol{\Sigma}\boldsymbol{V}^T \tag{8}$$

where $\boldsymbol{U}$ and $\boldsymbol{V}$ are the orthogonal matrix of $m \times m$ and $n \times n$ respectively, $\boldsymbol{\Sigma}$ is following.

$$\boldsymbol{\Sigma} = \left[\begin{array}{ccc|c} \sigma_1 & & O & \\ & \ddots & & O \\ O & & \sigma_m & \end{array}\right] \tag{9}$$

The singular values $\sigma_1,\ \sigma_2,\ \cdots, \sigma_m$ of $\boldsymbol{J}$ are arranged the square root $\sqrt{\lambda_i}$ of the characteristic value of $\boldsymbol{J}^T\boldsymbol{J}$ in order from large to small. When $i$th column vector of $\boldsymbol{U}$ is set to $\boldsymbol{u}_i$, the principal axis $\boldsymbol{m}_a$ of MEF is as follows.

$$\boldsymbol{m}_a = \boldsymbol{u}_1/\sigma_1,\ \boldsymbol{u}_2/\sigma_2,\ \cdots,\ \boldsymbol{u}_m/\sigma_m \tag{10}$$

### B. The Manipulating Force Ellipsoid in Consideration of Joint Torque

Because the MFE, as described in the preceding paragraph is based on the assumption that the maximum torque of each joint is a constant, and that there is also no difference by direction of positive and negative, it is necessary to include the difference in the torque based on the orientation and rotation direction in order to apply the concept to a person model. In the representation method of MFE in taking into consideration the joint torque asymmetry that has been proposed by Obinata et al. [13]. $\boldsymbol{f}_{\mathrm{mean}}$ is the center of the hand force.

$$(\boldsymbol{f} - \boldsymbol{f}_{\mathrm{mean}})^T\boldsymbol{J}\boldsymbol{J}^T(\boldsymbol{f} - \boldsymbol{f}_{\mathrm{mean}}) \leq 1 \tag{11}$$

(11) is normalized using (12) and (13), and the hand force set that fills $||\hat{\boldsymbol{\tau}} \leq 1||$ can be rewritten as (14).

$$\boldsymbol{T}_{\mathrm{r}} = \mathrm{diag}[1/(\tau_{i\mathrm{max}} - \tau_{i\mathrm{min}})] \tag{12}$$

$$\hat{\boldsymbol{J}} = \boldsymbol{J}\boldsymbol{T}_{\mathrm{r}} \tag{13}$$

$$(\boldsymbol{F} - \boldsymbol{F}_{\mathrm{mean}})^T\hat{\boldsymbol{J}}\hat{\boldsymbol{J}}^T(\boldsymbol{F} - \boldsymbol{F}_{\mathrm{mean}}) \leq 1 \tag{14}$$

An example of MFE when taking each joint torque into consideration is shown in Fig. 3. $(x_h, y_h)$ is hand position, $f_d$ is target force, $(x_v, y_v)$ is an intersection of a target force vector and MFE, $f_v$ is force which can be applied by a hand.

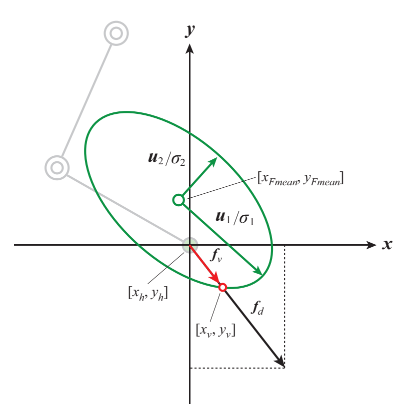


Fig. 3. Overview of the Manipulating Force Ellipsoid(MFE) considering each joint torque

### C. Analysis by the Manipulating Force Ellipsoid Consideration Joint Torque

The MFE of a healthy person and that of an individual with C5-level CCI was created. The results of calculating the MFE are shown in Fig. 4. The MFEs are normalized and denoted by the healthy person's maximum muscular force.

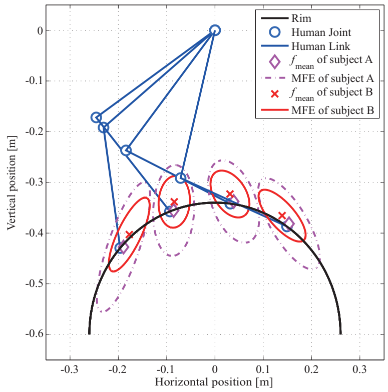


Fig. 4. Manipulating force ellipsoid (MFE): Participant A is able-bodied, Participant B has a C5-level cervical cord injury

The ellipses of an individual with C5-level CCI are about two thirds of a healthy person's ellipses. In addition, the position of $\boldsymbol{f}_{\mathrm{mean}}$ is far from the position of the hand, and the angle of the main radius of the ellipsoid is also different from the case of an able-bodied individual. Therefore, an individual with C5-level CCI can apply the force only about one fifth of the force of a healthy person at the time of extension with the largest difference. This signifies that an individual with C5-level CCI cannot apply an extension force to slightly inside of the tangential direction of the rim, since he cannot apply extending force of the elbow.

## IV. ASSISTANCE CONTROL IN WHEELCHAIR OPERATION

The analysis results of a previous chapter, indicates that the assistive power and assistive direction always change in wheelchair operation. Therefore, in order to assist with wheelchair operation, it is necessary to correctly interpret the motion of a wearer's arm and to understand the state of the wheelchair. A block diagram for this proposed method is shown in Fig. 5. A model taking into consideration both the wearer and the wheelchair was created, and driving force assistance to provide suitable timing according to a wearer's motion was rendered by allowing for correct interpretation of the current state. $F_M$ is the actual hand force, $F_E$ is the force added from the outside of the forearm, $F_F$ is the value of the pressure sensor of the forearm, and $F_G$ is the force required for wheelchair operation, $\hat{F}_M$ is the estimated hand force, $F_r$ is the assistive force, $F_d$ is the target force, $\theta_A$ is the angle of wearer's elbow, $\theta_R$ is the device's angle of the elbow and $\theta_d$ is the target angle.

First, the hand force was estimated from the flexion angle of the elbow and the angle of the shoulder. However, because only the angle of an elbow is output, the hand position and shoulder angle must be estimated from the elbow

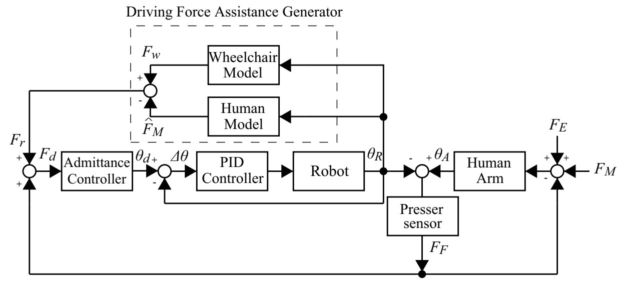


Fig. 5. Block diagram of the proposed method

angle. It therefore becomes possible to always correctly interpret the hand force during wheelchair operation. While the wheelchair velocity and acceleration are estimated, the torque and force required for target wheelchair velocity are derived. Insufficient driving force is assisted by comparing with the hand force estimated in advance.

### A. Estimated Method of Hand Force

In this chapter, we will explain the method for estimating hand force. In this research, the rigid model was composed of two links forming an upper arm and a front arm, and has two degree of freedom, a shoulder joint and an elbow joint, as shown in Fig. 6. This model was calculated on the $xy$ coordinates that are centered on the shoulder joint. Under ideal conditions, only sagittal plane is calculated because the elbow cannot move in a horizontal plane. $m_1$, $m_2$ are

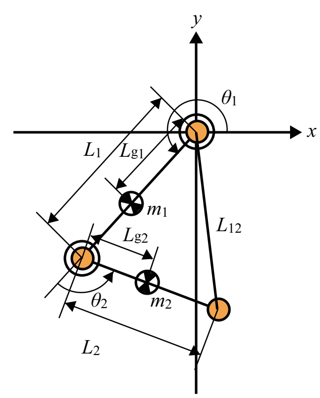


Fig. 6. Human model of two links

the masses of the forearm and the upper arm respectively, $L_1$, $L_2$ are the lengths of the forearm and the upper arm respectively, $L_{12}$ is the direct distance from the shoulder to the hand, $L_{g1}$, $L_{g2}$ are the lengths to the center of mass of the forearm and the upper arm respectively, and $\theta_1$, $\theta_2$ are the rotation angles of the forearm joint and the upper arm joint respectively. However, $\theta_1$ is a negative value.

The equation of motion for Fig. 6 is then derived using the Lagrange equation of motion.

$$\boldsymbol{M}(\boldsymbol{\theta})\ddot{\boldsymbol{\theta}} + \boldsymbol{h}(\boldsymbol{\theta}, \dot{\boldsymbol{\theta}}) + \boldsymbol{g}(\boldsymbol{\theta}) = \boldsymbol{\tau} \tag{15}$$

$$\boldsymbol{M}(\boldsymbol{\theta}) = \begin{bmatrix} M_{11} & M_{12} \\ M_{21} & M_{22} \end{bmatrix} \tag{16}$$

$$M_{11} = m_1 L_{g1}^2 + m_2 L_1^2 + m_2 L_{g2}^2 + I_1 + I_2 + 2m_2 L_1 L_{g2}\cos\theta_2 \quad (17)$$

$$M_{12} = M_{21} = m_2 L_{g2}^2 + I_2 + m_2 L_1 L_{g2}\cos\theta_2 \quad (18)$$

$$M_{22} = m_2 L_{g2}^2 + I_2 \quad (19)$$

$$\boldsymbol{h}(\boldsymbol{\theta}, \dot{\boldsymbol{\theta}}) = \begin{bmatrix} -m_2 L_1 L_{g2}(2\dot{\theta}_1 + \dot{\theta}_2)\dot{\theta}_2\sin\theta_2 \\ m_2 L_1 L_{g2}\dot{\theta}_1^2\sin\theta_2 \end{bmatrix} \quad (20)$$

$$\boldsymbol{g}(\boldsymbol{\theta}) = \begin{bmatrix} (m_1 L_{g1} + m_2 L_1)g\cos\theta_1 + m_2 L_{g2}g\cos(\theta_1 + \theta_2) \\ m_2 L_{g2}g\cos(\theta_1 + \theta_2) \end{bmatrix} \quad (21)$$

The torques of the shoulder joint and elbow joint are calculated using the above equation. In addition, there is the following relation between the hand force and the joint torque.

$$\boldsymbol{F} = (\boldsymbol{J}^T)^{-1}\boldsymbol{\tau} \quad (22)$$

where $\boldsymbol{J}$ is the Jacobi matrix and calculated by equation(23).

$$\boldsymbol{J} = \begin{bmatrix} -(L_1\sin\theta_1 + L_2\sin(\theta_1+\theta_2)) & -L_2\sin(\theta_1+\theta_2) \\ L_1\cos\theta_1 + L_2\cos(\theta_1+\theta_2) & L_2\cos(\theta_1+\theta_2) \end{bmatrix} \quad (23)$$

The degree of the shoulder angle is needed for estimating the hand force. The previously reported estimation method for determining the hand position and the degree of shoulder angle were used. The motion of a wearer's arm during wheelchair operation is modeled, as shown in Fig. 7, in consideration of the position of the rim of the wheelchair.

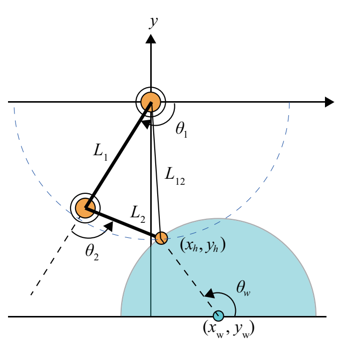


Fig. 7. Human model of wheelchair operation

When the angle of an elbow can be detected, the distance $L_{12}$ from a shoulder joint to a hand can be uniquely determined from (24).

$$L_{12} = \sqrt{(L_1 + L_2\cos\theta_2)^2 + (L_2\sin\theta_2)^2} \quad (24)$$

$L_{12}$ becomes the radius of the circle centering on a shoulder joint, and the hand position can be obtained from the intersection with the radius of a rim.

$$\begin{cases} x^2 + y^2 = L_{12}^2 \\ (x - x_w)^2 + (y - y_w)^2 = r_w^2 \end{cases} \quad (25)$$

where $x_w$, $y_w$ is the rim center and $r_w$ is the radius of the rim.

(26) will be obtained by adding (24) and (25), and solving simultaneous equations.

$$x_w x + y_w y - \frac{x_w^2 + y_w^2 + L_{12}^2 - r_w^2}{2} = 0 \quad (26)$$

The hand position$(x_h, y_h)$ is obtained by (26).

$$\begin{cases} x_h = \frac{x_w O_3 \pm y_w\sqrt{-O_3^2 + y_w^2 L_{12}^2 + x_w^2 L_{12}^2}}{(x_w^2 + y_w^2)} \\ y_h = \sqrt{L_{12}^2 - x_h^2} \\ O_3 = \frac{x_w^2 + y_w^2 + L_{12}^2 - r_w^2}{2} \end{cases} \quad (27)$$

Because (27) is the solution of the quadratic equation, $x_h$ is found at both positive and negative values. An intersection point of the circle is obtained for one or two point. From the characteristic features of a wheelchair, the point nearer to the shoulder side is also the hand position during flexion movement of the elbow, and the point nearer to the center of rim is the hand position during extension movements of the elbow. A negative value is therefore used during flexion motion, and positive value is used during extension motion.

If the hand position $(x_h, y_h)$ can be obtained, the angle of the shoulder joint can be obtained using (28) from the relation of inverse kinematics.

$$\theta_1 = -\arcsin\left(\frac{L_2\sin(\theta_2)}{\sqrt{x_h^2 + y_h^2}}\right) - \arctan\left(-\frac{y_h}{x_h}\right) \quad (28)$$

*B. Determination of the Amount of Assistance During Wheelchair Operation*

The rotation velocity of the wheelchair is calculated from the elbow angle during the flexion motion of the elbow being (29). The maximal velocity at that time is then considered for the target rim velocity $\theta_d$ during the extension motion of the elbow.

$$\dot{\theta}_{wf} = \tan\left(\frac{\dot{x}_{hf}}{\dot{y}_{hf}}\right) \quad (29)$$

where $(x_{hf},\ y_{hf})$ uses the negative value of (27).

The rotation velocity of the rim is then calculated from the hand position estimated as in (29) also during the extension motion. The required rim velocity is computed as compared with the rotation velocity of the target rim. The required driving force is obtained from (30). The difference between the necessary assisted force and the hand force estimated in the previous chapter is calculated.

$$T = I\dot{\omega} \quad (30)$$

$$\omega = \dot{\theta}_d - \dot{\theta}_{we} \quad (31)$$

where $T$ is the torque, $I$ is the moment of inertia and $\theta_{we}$ is the rim rotation velocity during extension motion of the elbow. The required impelling force is introduced from (30).

$$F_d = M_a r_w \dot{\omega} \quad (32)$$

This value and the hand force calculated previously are configured, and difference is considered to be the required assistive force.

*C. Verification Experiment by an Individual with C5-level CCI on the Floor*

A wheelchair operation was performed on the floor with the device attached. The subject was a male in his 30s with C5-level CCI. The running distance was set to 2.0 [m], and each experiment was conducted 3 times. The subject ran 2 m on the floor from a stop state. Then he was returned to the start position by a cooperator of the experiment. He ran 2 m again. The wheelchair operation was tracked by motion capture, and the wheelchair velocity was measured by color marking that was attached to the axle.

The running times with and without assist are shown in Table II, and one of the experimental results are shown in Fig. 8. From the top sequentially, the elbow angle, the angular velocity of the elbow, the assist force, the wheelchair velocity, and the wheelchair acceleration are shown.

TABLE II

DRIVE TIME OF 2.0[M]

| | Without assist [s] | With assist [s] |
|---|---|---|
| 1 | 5.22 | 4.43 |
| 2 | 5.83 | 4.86 |
| 3 | 5.80 | 4.26 |

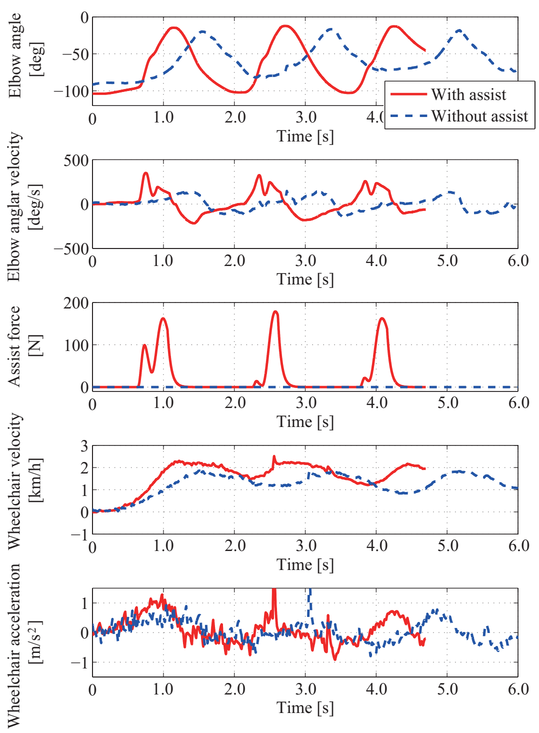


Fig. 8. Experimental results for wheelchair operation with C5-level CCI on the floor

From Fig. 8, it can be seen that in case with assistance, as compared with the case without, the velocity of the wheelchair is greater. In particular, the acceleration from a full stop becomes large and the maximum velocity of the wheelchair is also large due to the greater acceleration. In addition, the faster acceleration is maintained by subsequent operation. The running time for the measurement section is also short due to the high average velocity. As shown in Table II, the running time is approximately 1.0 [s] quicker for the 2.0 [m] run. Moreover, the number of times the wheelchair must be manipulated is decreased. With assistance, the wheelchair operator can move over the same distance more quickly with a smaller number of times of operation. The device provides more efficiency to the user by allowing a larger range of motion to push the wheel.

## V. CONCLUSIONS

In the present study, we developed a driving force assistance control system for wheelchair operation for individuals with C5-level CCI. Analysis of wheelchair operation for an individual with C5-level CCI was conducted. We confirmed that the rim could not be pushed out due to an insufficient extension force. The wearer's arm was modeled as a two-link manipulator, and the extension force and hand position were estimated using the equation of motion. The estimated extension force was compared with driving force required to operate a wheelchair with the target velocity defined at the time of arm flexion. We developed a system that assists with the problem of insufficient driving force. A verification experiment for wheelchair operation by an individual with C5-level CCI was conducted. In the experiment on the floor, the velocity and acceleration were increased, thus proving the validity of the proposed method.

## REFERENCES


[1] M.Hassan, H.Kadone, K.Suzuki, and Y.Sankai, Exoskeleton Robot Control based on Cane and Body Joint Synergies, Pro. of the 2012 IEEE/RSJ IROS, pp.1609-1614, 2012.

[2] E.Yagi, D.Harada and M.Kobayashi, Development of an Upper Limb Power Assist System using Pneumatic Actuators for Farming Lift-up Motion, Journal of System Design and Dynamics, Vol.3(No.5) , pp.781-791 , 2009.

[3] K.Kiguchi, Y.Hayashi, Adaptive Perception-Assist to Various Tasks for an Upper-Limb Power-Assist Exoskelton Robot, Proc. of IEEE SMC, pp.717-722, 2011.

[4] S. Marcheschi, F. Salsedo, M. Fontana, and M. Bergamasco, "Body extender: whole body exoskeleton for human power augmentation", In Proc. IEEE ICRA Annual Int. Conf., pp. 611-616, 2011.

[5] W. Yu, J.Rosen and X.Li, PID Admittance Control for an Upper Limb Exoskeleton, 2011 American Control Conference, pp.1124-1129, 2011.

[6] N.Vitiello, T.Lenzi, S.Roccella, S.M.M.De Rossi, E.Cattin, F.Giovacchini, F.Vecchi, M.C.Carrozza, "NEUROExos:A Powered Elbow Exoskeleton for Physical Rehabilitation", Robotics, vol. 29, no. 1, pp. 220-235, 2013.

[7] M.G. Carmichael and D.Liu, "Experimental evaluation of a model-based assistance-as-needed paradigm using an assistive robot", Proc. of IEEE EMBC, pp.866-869, 2013.

[8] Y.Mao, S.K.Agrawal,"Transition from Mechanical Arm to Human Arm with CAREX: a Cable Driven ARm EXoskeleton (CAREX) for Neural Rehabilitation", In Proc. IEEE ICRA Annual Int. Conf., pp. 2457-2462, 2012.

[9] T.D.Lalitharatne, Y.Hayashi, K.Kiguchi, "Compensation of the effects of muscle fatigue on EMG-based control using fuzzy rules based scheme", Proc. of IEEE EMBC, pp.6949-6952, 2013.

[10] A.Morbi, M.Ahmadi, D.C.Chan, R.Langlois, Comparing Continuous and Intermittent Assistance Controllers for Assistive Devices, Proc. of IEEE ICRA, pp.1419-1426, 2011.

[11] H.Weiguang, H.Jian, W.Yongji, W.Jun, C.Lei, Control of Upper-Limb Power-Assist Exoskeleton Based on Motion Intention Recognition, Proc. IEEE ICRA, pp. 2243-2248, 2011.

[12] R. Koeppe and T. Yoshikawa, Dynamic manipulability analysis of compliant motion, Proc. IEEE Int. Conf. on Intelligent Robots and Systems, Grenoble , France, pp.472-1478, 1977.

[13] M. Sasaki, T. Iwami, K. Miyawaki, I. Sato, G. Obinata and A. Dutta, Higher Dimensional Spatial Expression of Upper Limb Manipulation Ability based on Human Joint Torque Characteristics, Robot Manipulators New Achievements, pp.693-718,Intech,Publishing, 2010.

[14] N.Mizutani, T.Watanabe, N.Kato, K.Yano, T.Aoki, Y.Nishimoto and Y.Kobayashi, "A Wheelchair Operation Assistance Control for Wearable Robot Using with User's Residual Function", International Conference on Rehabilitation Robotics, 2013.